JACS
JOURNAL OF THE AMERICAN CHEMICAL SOCIETY
Article
pubs.acs.org/JACS

Nanomolar E-Selectin Antagonists with Prolonged Half-Lives by a Fragment-Based Approach

Jonas Egger,[#] Céline Weckerle,[#] Brian Cutting, Oliver Schwardt, Said Rabbani, Katrin Lemme, and Beat Ernst*

Institute of Molecular Pharmacy, Pharmacenter, University of Basel, Klingelbergstrasse 50, CH-4056 Basel, Switzerland

Supporting Information

ABSTRACT: Selectins, a family of C-type lectins, play a key role in inflammatory diseases (e.g., asthma and arthritis). However, the only millimolar affinity of sialyl Lewis^x (sLe^x), which is the common tetrasaccharide epitope of all physiological selectin ligands, has been a major obstacle to the development of selectin antagonists for therapeutic applications. In a fragment-based approach guided by NMR, ligands binding to a second site in close proximity to a sLe^x mimic were identified. A library of antagonists obtained by connecting the sLe^x mimic to the best second-site ligand via triazole linkers of different lengths was evaluated by surface plasmon resonance. Detailed analysis of the five most promising candidates revealed antagonists with K_D values ranging from 30 to 89 nM. In contrast to carbohydrate−lectin complexes with typical half-lives ($t_{1/2}$) in the range of one second or even less, these fragment-based selectin antagonists show $t_{1/2}$ of several minutes. They exhibit a promising starting point for the development of novel anti-inflammatory drugs.

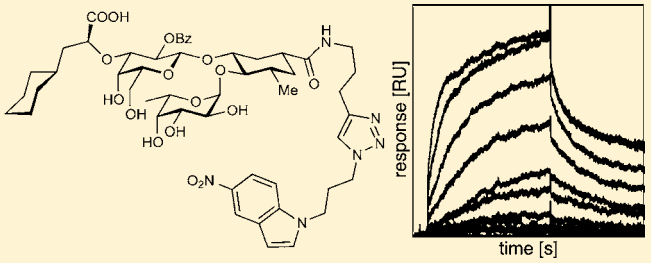

INTRODUCTION

In the last two decades, carbohydrate/lectin interactions were intensively studied,[1a] and their role as potential targets in numerous diseases was revealed.[1b,c] A prominent example is the selectins, which are involved in the extravasation of leukocytes from the bloodstream into surrounding tissues, a crucial step in inflammation. Selectins are a family of calcium-dependent lectins (E-, L-, and P-selectin) and mediate the first step in this process: the tethering and rolling of leukocytes on the endothelial surface.[2] This step is a prerequisite for their subsequent firm attachment mediated by the interaction of activated integrins and members of the IgG superfamily. In the final step, leukocytes extravasate and migrate to the site of inflammation.

This inflammatory cascade is forming a vital defense mechanism in the event of injuries and infections. However, excessive infiltration of leukocytes into adjacent tissue leads to its destruction and is therefore deleterious, as has been observed in many inflammatory diseases, such as myocardial ischemia reperfusion injury, asthma, and rheumatoid arthritis. In these cases, E-selectin mediated recruitment of leukocytes is associated with the etiology or progression of the disease.[1b] Furthermore, tumor cells use the selectin pathway to extravasate from the bloodstream to form metastases.[3] E-selectin antagonists therefore feature an untapped potential in treating inflammatory and related diseases as well as cancer.[1b,3] A recent example is the pan-selectin antagonist GMI-1070,[4] which was shown to reverse acute vascular occlusion in sickle cell mice.[5] It has successfully completed clinical phase 1 studies, and its efficacy is currently being investigated in humans with sickle cell disease.[6]

Sialyl Lewis^x (**1**, sLe^x, Figure 1) is the minimal carbohydrate epitope recognized by E-selectin.[7] The sLe^x/E-selectin interaction is characterized by low affinity ($IC_{50} \approx 1$ mM)[8] and a short half-life ($t_{1/2}$) in the range of seconds,[1b] one reason for this being the shallow and solvent-accessible binding site of E-selectin. While this behavior is necessary for selectin's physiological function,[9] it is a challenge for the development of selectin antagonists for therapeutic applications. Although numerous contributions presenting mimetic structures with considerably improved affinities have been published,[10] E-selectin antagonists with high affinities and slower dissociation rates[11] are still required.

The concept of fragment-based drug discovery (FBDD) represents a paradigm shift.[12a−e] One of the most striking features of FBDD is the fact that potent ligands can be obtained from low-affinity fragments, provided they are properly linked. The observed high affinity can be rationalized by the additivity of intrinsic binding energies of the fragments[13] and the reduction of translational and rigid-body rotational entropy costs upon fragment linking.[14] Fragment screens can be performed using readily available analytical technologies, e.g., nuclear magnetic resonance (NMR),[12f−i] X-ray crystallography,[12h,j] and surface plasmon resonance (SPR).[12k] Finally, suitable linkers can be identified by various procedures, e.g., by (i) rational design, (ii) the *in situ* click chemistry approach as

Received: March 24, 2013
Published: June 6, 2013

   dx.doi.org/10.1021/ja4029582 | J. Am. Chem. Soc. 2013, 135, 9820−9828

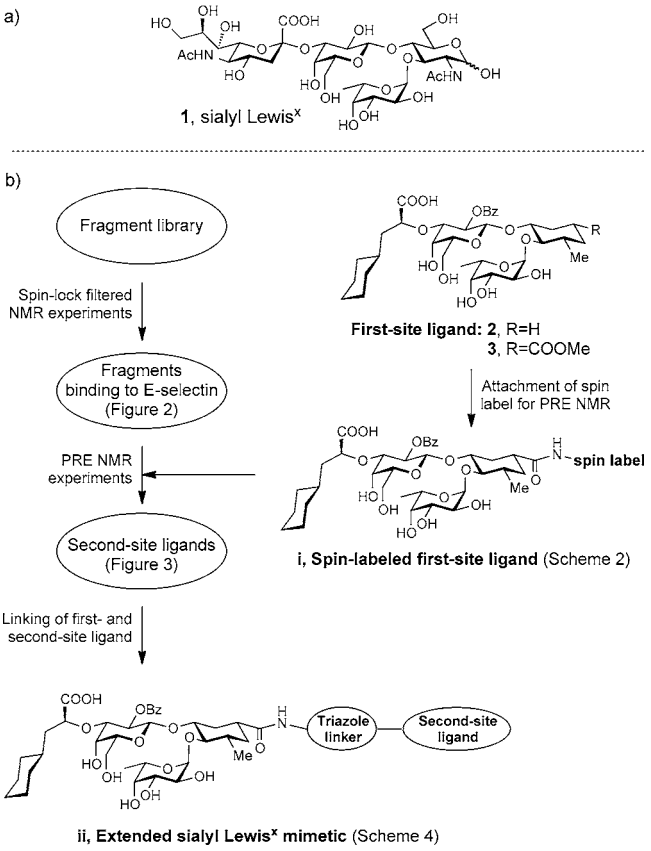

Figure 1. (a) Structure of sialyl Lewis^x (**1**). (b) A fragment library is screened for E-selectin binding using spin-lock filtered NMR experiments. Glycomimetics **2**[10f] and **3** represent first-site ligands. Those fragment hits binding in the proximity of the spin-labeled glycomimetic **3** (→ **i**) are identified by PRE NMR experiments and represent second-site ligands. In the last step, the sLe^x mimetic **3** is linked to a second-site ligand by [3 + 2]-Huisgen cycloaddition (→ **ii**).

described by Sharpless and co-workers,[15] or (iii) synthesis and biological screening of a classical compound library.

Recently, we reported a fragment-based approach for the discovery of potent ligands for the myelin-associated glycoprotein (MAG), a member of the sialic acid binding immunoglobulin-like lectin family (Siglecs).[16] A similar approach was employed by Balogh et al. for deducing ligand binding to gp41.[12g] Similar to MAG, the identification of selectin antagonists is impeded by the challenge of a shallow, unstructured binding site.[17] With a fragment-based approach, we planned to identify fragments binding adjacent to the carbohydrate recognition domain (CRD) of E-selectin. By linking these fragments with a mimetic of the physiological carbohydrate epitope sLe^x, high-affinity selectin antagonists are envisaged.

RESULTS AND DISCUSSION

The starting point in our search for high-affinity E-selectin antagonists was the sLe^x mimic **2**, which exhibits low micromolar affinity for the CRD of E-selectin (Figure 1).[10f]

In a first step, a fragment library was screened by NMR to identify ligands binding to E-selectin. These ligands were detected based on accelerated transverse magnetization decay in spin-lock filtered NMR experiments.[18] In a second step, these hits were subjected to paramagnetic relaxation enhancement (PRE) experiments in the presence of the spin-labeled first-site ligand **i**.[19] Those fragments binding in the vicinity of **i** are identified by PRE NMR experiments and represent second-site ligands. Furthermore, the distance dependence of the PRE was exploited to obtain information on the relative orientation of the second-site ligands with respect to the first-site ligand.[20] In the last step, a [3 + 2]-Huisgen cycloaddition[21] of azides and alkynes was applied in order to link the first-site ligand **3** with the second-site ligands (→ **ii**) (Figure 1). An inherent characteristic of this fragment-based strategy is its independence of structural information on the target protein.

Screening for Ligands. An in-house fragment library composed of 80 water-soluble molecules obeying the "Rule of Three"[22] ($M_W \leq 300$, clogP ≤ 3, number of hydrogen-bond donors ≤ 3 and acceptors ≤ 3) was screened by NMR. Prior to screening, the library was divided into sublibraries according to two criteria: First, six to eight components that do not interact/react with each other were pooled. Second, in the ^{1}H NMR spectrum of the sublibraries, each component has to be identifiable by at least one isolated resonance.

Binding to E-selectin was detected in so-called relaxation-edited or spin-lock filtered NMR experiments. These experiments are based on the fact, that the transverse relaxation of a molecule is related to its molecular weight. Nuclei in large molecules, such as proteins, exhibit fast magnetization decay compared to those in small molecules. When small molecules bind to a protein they adopt the relaxation properties of the protein as will become evident from a signal intensity reduction of the small molecule. This property can be exploited to identify ligand binding[23] by measuring the signal intensity of selected protons at different relaxation times in the absence and presence of E-selectin. With this approach, five fragments of the library were identified as binders to E-selectin: 5-nitroindole (**4**) (for an example of the experimental outcome, see Figure 3a,b), the benzimidazole derivative (**5**), 3-phenylpyrazol (**6**), benzothiazolone (**7**), and [1,1′-biphenyl]-4-methanol (**8**) (Figure 2).

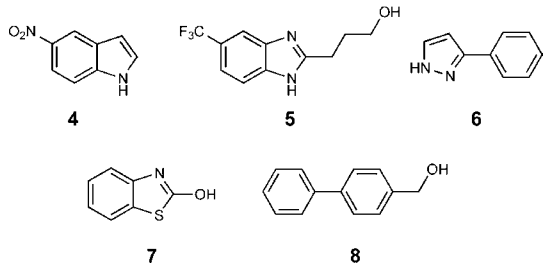

Figure 2. Ligands **4**–**8** identified by NMR screening of a fragment library.

Synthesis of the Spin-Labeled First-Site Ligand. To introduce the spin label and to subsequently link the first-site ligand with the second-site ligands, the sLe^x mimic **2**[10f] was equipped with a methyl ester (→ **3**, Figure 1). Docking studies and structural information from the crystal structure of E-selectin soaked with sLe^x (**1**)[17] suggested that the methyl ester in **3** is positioned in a nonbinding, sterically not restricted region and therefore is suitable for the introduction of the 2,2,6,6-tetramethylpiperidin-1-oxyl (TEMPO) spin label (→ **18•**) as well as for the attachment of a second-site ligand (see below).

To synthesize GlcNAc mimic **11** (Scheme 1), we started from commercial *cis*-1,2,3,6-tetrahydrophthalic anhydride (**9**),

dx.doi.org/10.1021/ja4029582 | J. Am. Chem. Soc. 2013, 135, 9820–9828

Scheme 1[a]

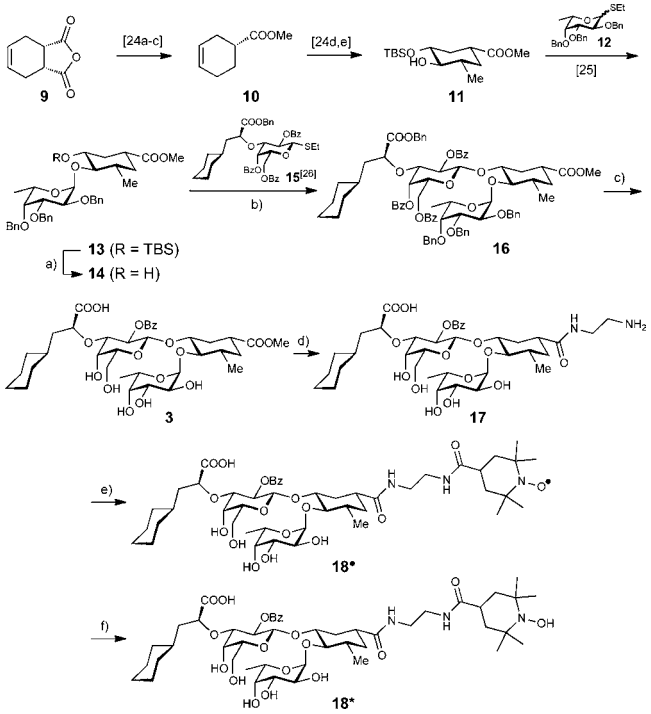

[a](a) TBAF, THF, rt, 13 h (76%); (b) DMTST, MS 4 Å, DCM, rt (80%); (c) i: Pd(OH)2/C, H_2, dioxane/H_2O; ii: NaOMe, MeOH (71%); (d) ethane-1,2-diamine, 65−70 °C, 2 h (93%); (e) HBTU, HOBt, 4-carboxy-TEMPO, DIPEA, DMF, rt, 1 h (48%); (f) Na-L-ascorbate, MeOH, rt, 1 h (68%).

which was transformed into (*R*)-cyclohex-3-ene carboxylic acid (**10**) with an enantiomeric excess of 96.3% ee, determined by chiral GC.[24a−c] Starting from **10**, methyl (1*R*,3*R*,4*R*,5*S*)-3-(*tert*-butyldimethylsilyloxy)-4-hydroxy-5-methyl-cyclohexane-1-carboxylate (**11**) was obtained according to a described sequence.[24d,e] α-Fucosylation[25] (→ **13**) followed by desilylation yielded the glycosyl acceptor **14**. Its glycosylation with donor **15**[26] and dimethyl(methylthio)sulfonium triflate (DMTST) as a promoter provided the pseudotetrasaccharide **16** with β-selectivity. Hydrogenolysis of the benzyl groups with $Pd(OH)_2/C$ and saponification under Zemplén conditions yielded the 2-monobenzoylated antagonist **3**.

Because direct aminolysis of ester **3** with 4-amino-TEMPO yielded only trace amounts of the corresponding amide, a diaminoethane spacer was introduced (→ **17**). Amine **17** was then coupled to 4-carboxy-TEMPO using HBTU/HOBt for activation to yield the spin-labeled, first-site ligand **18•**. To obtain high-resolution NMR spectra, oxyl **18•** was reduced to hydroxide **18*** by adding Na-L-ascorbate.

Biological Evaluation. The interaction between the antagonists **2**, **3**, and **18•** and E-selectin/IgG fusion protein was analyzed by SPR at 25 °C.[27] Between 6000 and 7000 RU of E-selectin/IgG, for preparation and purification see Experimental Section, were immobilized on the chip surface via a polyclonal goat antihuman Fc antibody as described in the Experimental Section. A flow cell providing only the antibody was used as reference. Dilution series of the first-site ligands **2**, **3**, and **18•** were prepared from stock solutions in DMSO using HBS-P buffer (0.01 M HEPES, 0.15 M NaCl, 0.005% surfactant P20 [pH 7.4]). Neither the introduction of the ester (antagonist **3**) nor the TEMPO moiety (antagonist **18•**) had a substantial effect on the affinity or the kinetic profile of these first-site ligands (Table 1).

Table 1. Kinetic and Affinity Evaluation of the Best-Ranked Triazole-Nitroindole Antagonists, i.e., 35, 41, 43, 45, and 51 and the Precursors 2, 3, and 18• From SPR Experiments[a]

entries	analyte	$K_{D,eq}$ [μM]	$K_{D,k_{in}}$ [μM]	k_{on} [10^5 $M^{-1}s^{-1}$]	k_{off} [s^{-1}]	$t_{1/2}$ [s]
1	**2**	1.45	1.0	8.5	0.9	0.77
2	**3**	1.90	1.7	11	1.9	0.37
3	**18•**	1.25	1.2	3	0.36	1.9
4	**26b**	1.12	1.12	35.4	3.98	0.174
5	**35**	0.089	0.036	0.635	0.0023	301
6	**41**	0.057	0.037	0.68	0.0025	280
7	**43**	0.030	0.018	1.42	0.0026	250
8	**45**	0.049	0.035	0.797	0.0028	240
9	**51**	0.050	–	–	–	–
10	**53**	0.186	0.189	0.3	0.0056	124
11	**58**	0.544	–	–	–	–

[a]$K_{D,eq}$ is obtained from a steady-state fit of the equilibrium responses to a single binding site model; k_{on} and k_{off} were obtained from curve fitting to the association and dissociation phases, respectively; $K_{D,k_{in}}$ was calculated from k_{off} and k_{on} using $K_D = k_{off}/k_{on}$; $t_{1/2}$ is calculated from k_{off} using $t_{1/2} = \ln 2/k_{off}$.

Identification of Fragments That Bind Adjacent to the First-Site Ligand (Second-Site Fragments). In the next step, the spin-labeled antagonist **18•** was used to identify fragments that bind simultaneously and in the vicinity of the sLe^x-binding site. Since the gyromagnetic ratio of an unpaired electron is 658 times larger than that of a proton, the TEMPO spin label dramatically enhances the rate of transverse relaxation of surrounding protons within a radius of ~10 Å.[28] This phenomenon, called paramagnetic relaxation enhancement (PRE), is distance dependent and thus allows the identification of fragments that bind in the vicinity of the first-site ligand and therefore represent second-site ligands. As illustrated in Figure 3c, the addition of **18•** further reduced the signal intensity of **4** compared to the situation when only E-selectin is present (Figure 3b), suggesting simultaneous binding and proximity of **4** and **18•**. To ensure that the observed effect was truly the result of the spin label, we reduced the radical **18•** by adding Na-L-ascorbate to the NMR sample (→ **18***). Indeed, this canceling of the paramagnetic effect led to an almost complete recovery of the signal (Figure 3d). Corresponding experiments were performed with the other second-site ligands **5**−**8**. In this process, **5** was also confirmed to be a second-site ligand binding to E-selectin in the vicinity of the first-site ligand.

In contrast, the presence of **18•** did not cause PRE for the ligands **6**−**8**, indicating that these ligands are not second-site binders to E-selectin.

Orientation of the Second-Site Ligand. The distance dependence of the PRE of the radical **18•**[28] was further exploited to determine the orientation of the second-site ligand relative to the spin label, i.e., to the first-site ligand. We used the resonances of H-3, H-4, and H-7 of **4**, because they show no (H-3 and H-4) or only minimal (H-7) overlap with resonances of **18•**. The differences in the relaxation rates (Δ-values in Figure 4) obtained in the presence of **18•** or **18*** indicate that H-7 is located closer to the radical than H-3 and H-4. For the benzimidazole derivative **5**, the orientation cannot be

dx.doi.org/10.1021/ja4029582 | J. Am. Chem. Soc. 2013, 135, 9820−9828

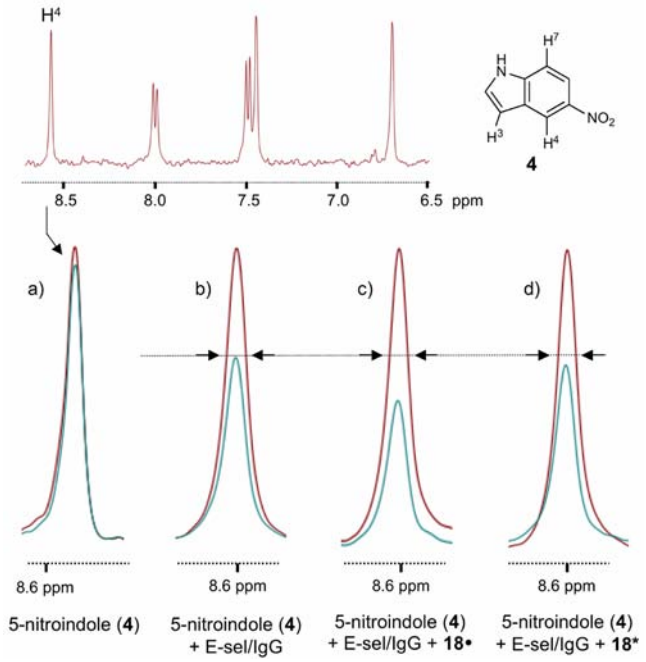

Figure 3. Principle of screening for second-site ligands. ^{1}H NMR spectra of H-4 of **4** recorded at spin lock times of 10 ms (red spectra) and 200 ms (green spectra) in different NMR samples: (a) **4** in solution; (b) addition to E-selectin/IgG causing transverse relaxation enhancement at longer spin-lock times; (c) addition of **18•** causing PRE; (d) addition of Na-L-ascorbate leading to a reduction of **18•** to **18*** and a reversal of PRE.

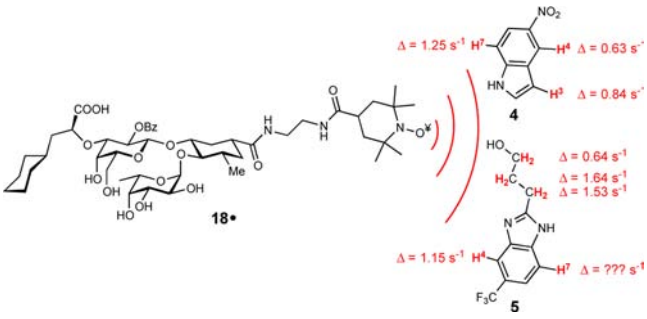

Figure 4. Relative orientation of the second-site ligands with respect to the spin-labeled first-site ligand **18•**. The increase in transversal relaxation rates (Δ) experienced upon addition of **18•** to a mixture of **4** or benzimidazole **5** with E-selectin/IgG reflects the distance of a nucleus to the unpaired electron.

determined unambiguously, due to the inability to quantify a relaxation rate for H-7 and the conformational flexibility of the hydroxypropyl side chain.

Synthesis of First-Site Ligands with Different Linkers. The synthesis of the trimethylsilyl-protected amines **23a−d** started from the corresponding alcohols **20a−d**. Whereas **20a−c** are commercially available, **20d** was obtained by silylation of hex-5-yn-1-ol (**19**) (Scheme 2). Mesylation (→ **21a−d**) and substitution by azide (→ **22a−d**) yielded, after reduction under Staudinger conditions, the amines **23a−d**. In contrast to the treatment with diaminoethane (**3** → **12**, Scheme 1), direct aminolysis of **3** with the alkyne amines **23a−d** yielded the amides **25a−d** only in moderate yields (2−18%). A possible reason for this is the low stability of the amines **23a−d** at elevated reaction temperatures (65−130 °C), leading to

Scheme 2. [a]

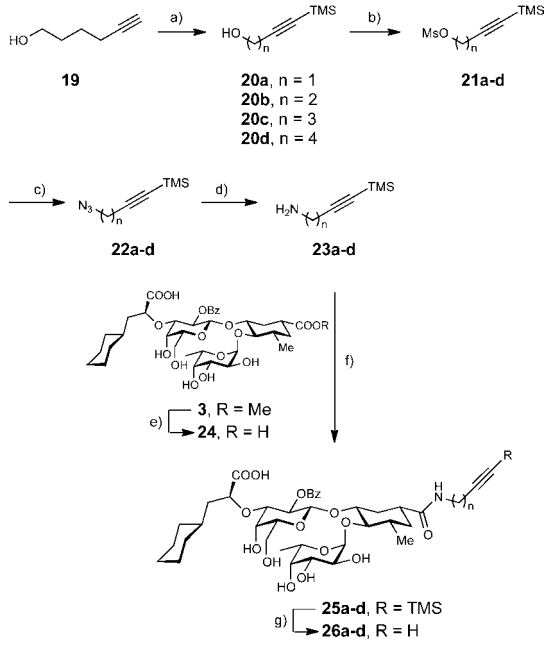

[a](a) ^{t}BuLi, Me_3SiCl, THF, −90 to −10 °C; (b) $MeSO_2Cl$, Et_3N, DCM, −78 °C to rt; (c) NaN_3, DMF, 65 °C; (d) PPh_3, THF/H_2O, 50 °C (**23a**: 83% for 3 steps; **23b**: 80% for 3 steps; **23c**: 43% for 3 steps; **23d**: 62% for 4 steps); (e) NaOH, MeOH/H_2O, rt (79%); (f) i: HBTU (1.2 equiv), HOBt (3 equiv), DMF; ii: alkyne amine, rt (**25a**: 35%; **25b**: 70%; **25c**: 40%; **25d**: 44%); (g) TBAF, THF, rt (**26a**: 80%; **26b**: 93%; **26c**: 98%; **26d**: 87%).

polymerization after cleavage of the trimethylsilyl group. In addition, the electron-withdrawing effect of the acetylene reduces the nucleophilicity of the amino groups.

In an alternative approach, diacid **24** was selectively activated using standard peptide coupling conditions (HBTU and HOBt). The desired amides **25a−d** were obtained with excellent selectivity (93−99%) and fair to good yields (34−72%). Amides of the lactic acid moiety are formed only in trace amounts and were removed by conventional HPLC. The unexpected regioselectivity probably results from different reactivities/accessibilities of the two carboxylates in **24**, e.g., due to formation of intramolecular hydrogen bonds, steric constraints, and a reduced reactivity of the lactic acid moiety resulting from the electron-withdrawing oxygen in the α-position. Finally, cleavage of the trimethylsilyl groups with tetrabutylammonium fluoride (TBAF) yielded the alkynes **26a−d**.

Synthesis of a Library of Extended sLe^x Mimics. Of the two second-site fragments, 5-nitroindole (**4**) and the benzimidazole **5**, the former offers synthetic advantages and does not contain a flexible side chain. In addition, its relative orientation versus the first-site ligand was able to be determined more reliably. This made indole **4** the molecule of choice for the synthesis of a second-site library.

According to the orientation of **4** toward the first-site ligand (see Figure 4), the azidoalkyl linkers were introduced by *N*-alkylation (→ **28a − d**, Scheme 3) and, for proof of concept, into the 3-position as well (→ **32a − d**, Scheme 3). *N*-alkylated 5-nitroindoles with 2-azidoethyl, 3-azidopropyl and 4-azidobutyl linkers were obtained by *N*-alkylation of **4** with the corresponding dibromoalkanes followed by nucleophilic

dx.doi.org/10.1021/ja4029582 | J. Am. Chem. Soc. 2013, 135, 9820−9828

Scheme 3[a]

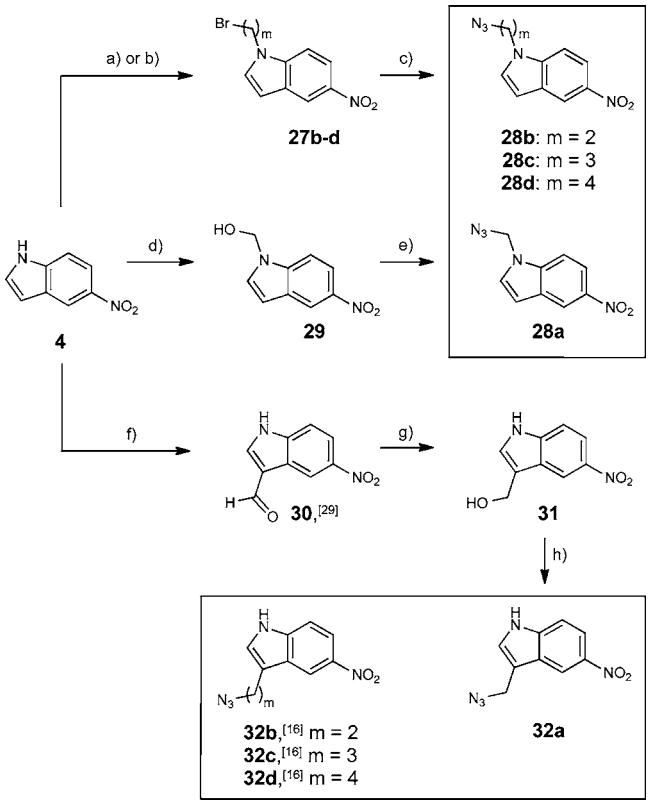

[a](a) $Br(CH_2)_2Br$ or $Br(CH_2)_3Br$, KOH, DMF, rt (**27b**: 19%; **27c**: 46%); (b) $Br(CH_2)_4Br$, K_2CO_3, TBAB, EtOAc, 50 °C (**27d**: 46%); (c) NaN_3, DMF, 60 °C (**28b**: 52%; **28c**: 82%; **28d**: 79%); (d) 30% aq. CH_2O, K_2CO_3, EtOH, 60 °C (66%); (e) i: $MeSO_2Cl$, Et_3N, THF, −15 °C to rt; ii: NaN_3, 15-crown-5, rt (34%); (f) $POCl_3$, DMF, −15 °C to rt (92%); (g) $NaBH_4$, MeOH, rt (92%); (h) DPPA, DBU, toluene/THF, −15 °C to rt (78%).

substitution with sodium azide (→ **28b−d**). For the introduction of the azidomethyl linker, hemiaminal **29** was synthesized from **4** and formaldehyde. Azide **28a** was obtained by *in situ* formation of the mesylate followed by nucleophilic substitution with sodium azide.

The *C*-alkylated 5-nitroindole **32a** was obtained via a Vilsmeier formylation of **4**[29] (→ **30**), followed by reduction to alcohol **31**, which was directly converted to azide **32a** using diphenylphosphoryl azide (DPPA).[30] The syntheses of the nitroindoles with 3-azidoethyl (→ **32b**), 3-azidopropyl (→ **32c**), and 3-azidobutyl (→ **32d**) linkers via a Larock indole synthesis[31] have been previously reported.[16]

***In situ* Click Experiments.** In a first attempt to identify a suitable linker to connect first- and second-site ligands, a series of *in situ* click experiments[15,16] were performed. However, despite careful optimization of the experimental conditions with regard to ligand and protein concentrations, no evidence of preferential formation of a specific linker combination was found. With its flat binding site, E-selectin does not act as an effective supramolecular catalyst for the alkyne−azide cycloaddition, because even upon simultaneous binding of first- and second-site ligand their azide- and acetylene-substituted linkers are not sufficiently preorganized to accelerate the cycloaddition reaction. Furthermore, the ligands' low affinities in the micromolar (first-site ligand) and millimolar (second-site ligand) range leads to a low concentration of ternary complex, thus aggravating the detection of catalytically formed triazoles.

Synthesis and Ranking of Triazole Antagonists. As the *in situ* click chemistry approach did not lead to the identification of a suitable linker pattern, a library of triazole antagonists[32] with different linker lengths was synthesized using the copper-catalyzed alkyne−azide cycloaddition reaction (CuAAC)[33] (Scheme 4).

Scheme 4[a]

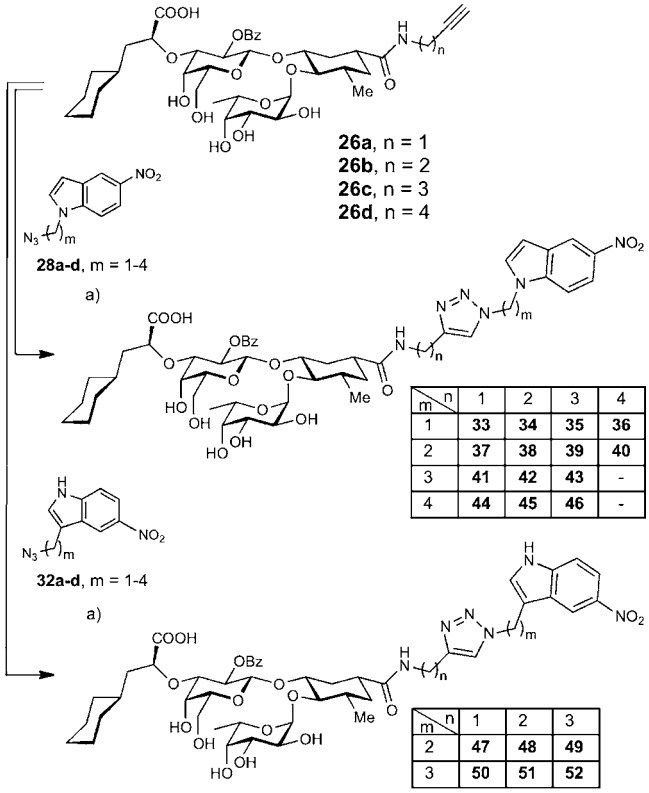

m \ n	1	2	3	4
1	33	34	35	36
2	37	38	39	40
3	41	42	43	-
4	44	45	46	-

m \ n	1	2	3
2	47	48	49
3	50	51	52

[a](a) Na-L-ascorbate, $CuSO_4 \cdot 5\ H_2O$, ^{t}BuOH/H_2O/THF, rt, 2−3 h (21−98%).

To rank the library members, SPR experiments with immobilized E-selectin/IgG were recorded at a single antagonist concentration (0.05 μM). Because for a biomolecular interaction the change in refractive index is proportional to the mass of the bound ligand, the measured intensities given in resonance units [RU] were normalized according to the molecular weight of the ligand (data not shown). Compared to the first-site ligand **2** (Table 1, entry 1), ester **3** (entry 2), the spin-labeled antagonist **18•** (entry 3) or the butynyl amide **26b** (entry 4) did not affect the binding parameters. However, 5 of the 20 tested antagonists (see Scheme 4) showed a distinctively strong intensity/molecular weight ratio and were therefore subjected to a comprehensive SPR evaluation to obtain K_D values as well as the on- and off-rates of binding. The nitroindole derivatives **35**, **41**, **43**, **45**, and **51** (entries 5−9) bind E-selectin with a 16- to 48-fold higher affinity (equilibrium K_Ds between 89 and 30 nM) compared to **2**. The order of affinities in the detailed analysis was the same as in the ranking procedure. In addition to the improved affinities, these antagonists also exhibited substantially improved binding kinetics, with ligand−receptor half-lives up to 4−5 min instead

dx.doi.org/10.1021/ja4029582 | J. Am. Chem. Soc. 2013, 135, 9820−9828

of the previously observed half-lives in the range of a second or even below (Figure 5).

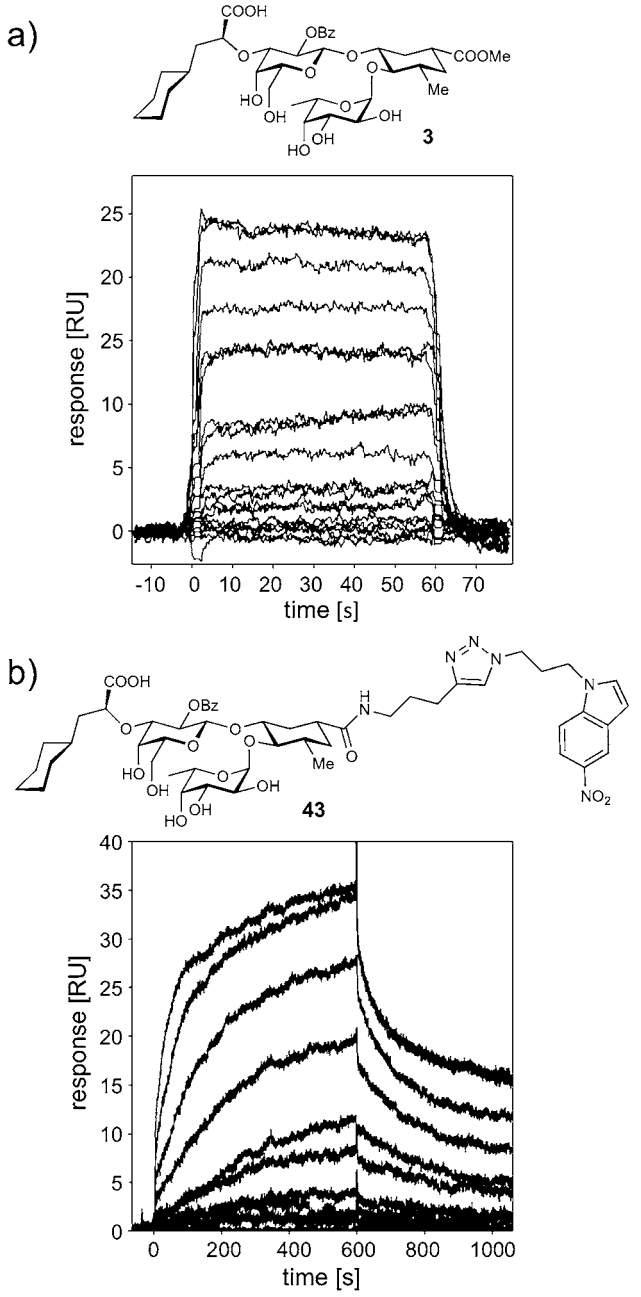

Figure 5. Sensorgrams of (a) the tetrasaccharide mimic **3**, with the characteristic block shape indicating fast on/off rates, and (b) the best triazole-nitroindole antagonist **43**.

All five antagonists that were comprehensively evaluated by SPR had rather long linkers containing four (**35** and **41**), five (**51**), or even six (**43** and **45**) methylene groups. **35**, **41**, **43**, and **45** contained an *N*-linked nitroindole, which supports the finding that the nitroindole binds preferentially with its indole nitrogen oriented toward the first-site ligand (see Figure 4). However, **51** represents a case where a favorable positioning of a *C*-linked nitroindole is also possible.

Tetrasaccharide mimics, such as **3**, interact with E-selectin mainly via a set of well-defined electrostatic interactions.[17] The high water accessibility of the binding site and the high degree of ligand preorganization allows for a fast exchange of solvent molecules by the ligands, which may be the cause of their typical fast association and dissociation.[2] In contrast, the prolonged association and dissociation phases seen for the triazole–nitroindole antagonists (Table 1, entries 5–8) indicate that the binding event might be accompanied by an induced fit of the ligand and/or the protein.[34] To resolve these structural issues, attempts to cocrystallize a high-affinity antagonist, e.g., **43**, with E-selectin have been initiated.

Derivatization of the Nitro Group. To estimate the toxic potential of the parent compound, the antagonist **43**, its affinity toward 16 proteins known or suspected to trigger adverse effects (10 nuclear receptors: AR, ERα, ERβ, GR, LXR, MR, PPARγ, PR, TRα, TRβ; four members of the cytochrome P450 enzyme family: 1A2, 2C9, 2D6, 3A4; hERG and the AhR) was simulated and quantified employing the VirtualToxLab[35] technology. The simulations suggest that **43** does not display any significant affinity (i.e., K_i < 100 μM) toward any of the tested proteins. However, since the metabolic biotransformation of nitro arenes involves several reactive intermediates (e.g., nitroso derivatives or hydroxyl amines) with toxic or mutagenic potential,[36] possible replacements for the nitro group were explored. Modifications leading to a decrease in lipophilicity appeared particularly interesting. Accordingly, starting from **43**, derivatives with a 5-aminoindole moiety (→ **53**) and the corresponding acetamide (→ **58**) were prepared (Scheme 5).

Scheme 5[a]

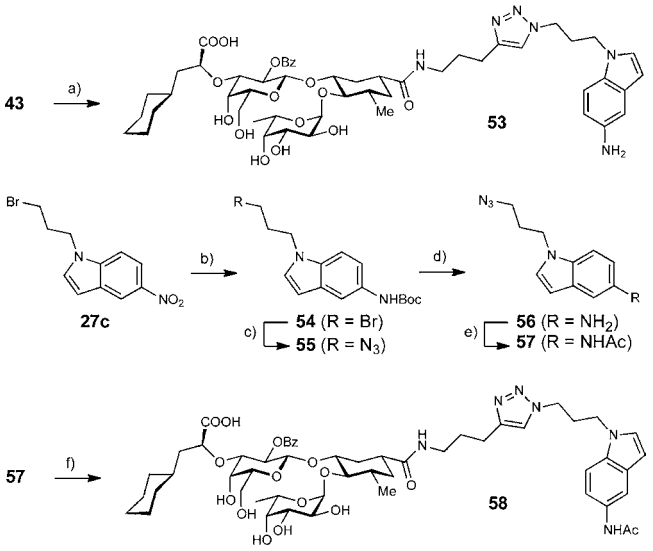

[a](a) PtO_2, H_2, morpholine, rt (54%); (b) PtO_2, H_2, Boc_2O, EtOH, rt (72%); (c) NaN_3, DMF, rt (90%); (d) TFA, DCM, rt (86%); (e) Ac_2O, Et_3N, DCM, rt (86%); (f) **26c**, Na-L-ascorbate, $CuSO_4 \cdot 5H_2O$, ^{t}BuOH/H_2O/THF, rt (73%).

The affinities of **53** and **58** are reported in Table 1. Surprisingly, the effect of the nitroindole modification on the affinity was quite strong. Compared to the parent compound **43**, the affinity of amine **53** (K_D = 186 nM) was reduced by a factor of 6 and for the acetamide **58** (K_D = 544 nM), by as much as a factor of 16. The 5-position of the indole is apparently crucial for binding of the second-site ligand. Although amines and amides are better hydrogen-bond acceptors than the nitro group,[37c] the orientation of their acceptor lone pairs differs. In addition, nitro groups may

dx.doi.org/10.1021/ja4029582 | J. Am. Chem. Soc. 2013, 135, 9820–9828

electrostatically interact with carbonyl groups that are oriented orthogonally or antiparallel to the plane of the nitro group.[37] Furthermore, unfavorable desolvation penalties may explain the reduced affinity of amine **53** and acetamide derivative **58**.[38]

■ CONCLUSIONS

We successfully screened a fragment library by NMR and identified 5-nitroindole (**4**) and benzimidazole **5** as second-site ligands binding in close proximity to the first-site selectin antagonist **2**. For synthetic and structural reasons, the indole derivative **4** was selected for further studies. Because linking of first- and second-site ligands by *in situ* click experiments[15,16] failed, a library consisting of 20 triazole derivatives with differing linker lengths was synthesized. The antagonists were ranked according to their relative affinities using SPR experiments. The five most potent antagonists (Table 1, entries 5−9) were subjected to a detailed analysis by SPR, revealing K_D values between 30 and 89 nM and a half-life of the ligand−protein complex in the range of 4−5 min. For E-selectin antagonists, this is a substantial improvement with respect to affinity as well as half-life, since carbohydrate−lectin interactions are generally characterized by micro- to millimolar affinities and half-lives in the range of seconds.[2]

As shown for antagonist **43**, the nitro group of the indole moiety is required for binding, and its replacement by an amino- (→ **53**) or acetamido group (→ **58**) led to a substantial loss of affinity. The second-site ligand improves binding ∼50-fold. Because the rather long linkers are flexible, a potential improvement in affinity can probably be achieved with linkers of reduced flexibility. Finally, the presented E-selectin antagonists have a pronounced amphiphilic nature. Therefore, the introduction of polarity into the linker might be beneficial in terms of solubility.

The development of high-affinity ligands for lectins in general and E-selectin in particular has proven to be a notoriously difficult task. E-selectin antagonists with low nanomolar affinities constitute a substantial step forward in the search for novel anti-inflammatory drugs and may foster a better understanding of binding processes at solvent exposed, extended, and flat binding sites. Especially for those antagonists where structural information on the target protein is missing and lead optimization using "conventional" approaches is only partially successful, the presented fragment-based lead optimization strategy offers novel opportunities to advance to drug-like affinities in the low nanomolar range.

■ EXPERIMENTAL SECTION

Synthesis. For experimental and spectroscopic details see Supporting Information.

NMR Screening. All NMR experiments were performed on a Bruker AVANCE III 500 MHz (Bruker BioSpin AG, Fällanden, Switzerland) equipped with a *Z*-gradient SEI probe at 298 K. Each NMR sample contained 0.5 mg/mL of E-selectin/IgG, equivalent to 15 μM of binding site (estimated by Bradford assay). The E-selectin/IgG was prepared in Tris-d_{11}-buffer (50 mM Tris-d_{11}, 150 mM NaCl, 1 mM $CaCl_2$). Shigemi NMR tubes (Sigma Aldrich GmbH, Buchs, Switzerland) were used for samples containing E-selectin/IgG (sample volume: 250 μL), and standard 5 mm NMR tubes were used for samples containing only ligands (sample volume: 500 μL). Bruker software XWINNMR 3.6 and TOPSPIN 2.1 were used. MestReNova 5.2.3 was used for off-line analysis of the NMR spectra. Prism 4 (GraphPad Software Inc., San Diego, U.S.A.) was used for nonlinear curve fitting of relaxation data.

Spin−Spin Relaxation Experiments. E-selectin/IgG was present at 20−30 μM in binding site concentration as determined by a Bradford assay. A 50 mM stock solution of compound in d_6-DMSO was prepared and diluted with deuterated buffer (pH 7.4, 20 mM Tris-d_{11}, 150 mM NaCl, 1 mM $CaCl_2$ in D_2O, Armar Chemicals) to a final sample concentration of 1−5 mM. The pulse sequence used for T1ρ spin-lock filtered experiments was adapted from Hajduk.[23] To determine the transversal relaxation rate, six experiments were performed with different durations of the continuous-wave spin-lock applied with a field strength of 2 kHz (10, 50, 100, 150, 200, 250 ms). The residual water signal was suppressed by a DPFGSE sequence added at the end of the pulse sequence.[39] For each experiment, eight scans were measured preceded by two dummy scans. The recovery delay between successive scans was set to 10 s, and the FID was digitally sampled for 2 s.[40]

Surface Plasmon Resonance (SPR) Analysis. Molecular interaction analyses by SPR were performed on a Biacore 3000 system (GE Healthcare, Uppsala, Sweden). CM5 research grade sensor chips, amine coupling immobilization kit, maintenance supply, and HPS-P buffer were purchased from GE Healthcare (Freiburg, Germany). HBS-P buffer (10 mM HEPES, 150 mM NaCl, 0.005% P20, pH 7.5) supplemented with 5% (v/v) DMSO (D8418, Sigma-Aldrich Chemie, Steinheim, Germany) and 20 mM $CaCl_2$ (C3306, Sigma-Aldrich, Steinheim, Germany) was used as running buffer in all binding experiments. The capture assay for the immobilization of E-selectin/IgG was performed as follows: A polyclonal goat antihuman Fc antibody (I2136, Sigma-Aldrich, Buchs, Switzerland) was first immobilized onto a CM5 sensor chip via the standard amine coupling method according to the manufacturers protocol. After antibody immobilization, a solution of E-selectin/IgG (50 μg/mL, in acetate buffer 10 mM, pH 5.5) was injected at 5 μL/min for 20 min on a single-flow cell. A reference cell without immobilized E-selectin/IgG was prepared. Before injecting the antagonist, the flow cells were equilibrated for 2 h in running buffer at 5 μL/min. For the evaluation of first-site ligands, serial dilutions were prepared in running buffer and injected using the KINJECT command with a 60 s association time and 60 s dissociation time at a flow rate of 20 μL/min over the reference and the active flow cell. Prior to each assay, a DMSO calibration was performed.[41] For the ranking of the triazole antagonists, the association and dissociation times were increased up to 600 s. SPR signals were recorded at a single concentration of ligand (50 nM, in running buffer) at a flow rate of 20 μL/min. The average of the signal recorded at 500 to 600 s after injection (plateau) was calculated and divided by the molecular weight of the analyte. To eliminate intensity differences resulting from the use of different chip batches and surfaces, the obtained results were normalized to the response of an internal standard (**46**) injected at a concentration of 50 nM. In addition, blank injections were performed between each injection of ligand to prevent the presence of residual traces of compound in the system. Similar conditions were applied for the K_D, k_{off}, and k_{on} determinations of the best antagonists, which were selected according to the data obtained by the ranking procedure. Ten dilutions were measured for each antagonist. The data were processed with Scrubber 2.0a (BioLogic Software, Campbell, Australia) for equilibrium binding constants (K_D) measurements and the determination of kinetic parameters (k_{on}, k_{off}). K_Ds were determined using a simple steady-state affinity 1:1 binding model. Double referencing (subtraction of reference surface and blank injection) was applied to correct bulk effects and other systematic artifacts.[42]

E-Selectin/IgG Expression and Purification.[10f] CHO-K1 cells expressing the E-selectin/IgG construct, which includes the lectin domain, the EGF-like domain, and six complement repeat domains of human E-selectin fused to the Fc part of human IgG1, were generated as previously described.[43] The cells were cultivated as monolayers at 37 °C, 5% CO_2, in F-12 culture medium supplemented with 10 mM sodium pyruvate, 10% FCS, 100 U/mL penicillin, 100 μg/mL streptomycin, and 0.4 mg/mL geneticin (G418) sulfate. For the expression, the cells were adapted to 5% FCS and αDMEM medium with the same additives as for the F-12 culture medium. Conditioned culture medium was harvested once a week and stored at −20 °C.

E-selectin/IgG was purified from the conditioned culture medium by affinity chromatography; first with protein A-Sepharose, followed by a second purification with the 7A9-Sepharose column (monoclonal anti hE-selectin antibody, ATCC no. HB-10135TM). Purified E-selectin/IgG was concentrated by ultrafiltration (1610g, Vivaspin 20, 50 kDa cut off) and dialyzed overnight against assay buffer (10 mM HEPES, 150 mM NaCl, 1 mM $CaCl_2$, pH 7.4) using Slide-A-Lyzer dialysis cassettes (cut off 10 kDa). The protein purity was confirmed by standard SDS-PAGE analysis, and the concentration was determined by HPLC-UV against a BSA standard.

■ ASSOCIATED CONTENT

Supporting Information

Synthesis and spectroscopic data; HR-MS and HPLC data for all target compounds; HPLC traces and ^{1}H NMR spectra for all target compounds. This material is available free of charge via the Internet at http://pubs.acs.org.

■ AUTHOR INFORMATION

Corresponding Author

beat.ernst@unibas.ch

Author Contributions

[#]These authors contributed equally.

Notes

The authors declare no competing financial interest.

■ ACKNOWLEDGMENTS

We gratefully acknowledge the financial support by the Swiss National Science Foundation (grant no. 200020-120628) and by GlycoMimetics Inc., Gaithersburg, MD (U.S.A.). The authors express their gratitude to Dr. Brigitte Fiege, Institute of Molecular Pharmacy, University of Basel for critical revision of the manuscript and also thank Mr. Werner Kirsch, Microanalytical Services of the Department of Chemistry of the University of Basel for performing the microanalyses.

■ REFERENCES

(1) (a) Gabius, H.-J.; André, S.; Jiménez-Barbero, J.; Romero, A.; Solís, D. *Trends Biochem. Sci.* **2011**, *36*, 298−313. (b) Ernst, B.; Magnani, J. L. *Nat. Rev. Drug Discovery* **2009**, *8*, 661−677. (c) Osborn, H. M. I.; Evans, P. G.; Gemmell, N.; Osborne, S. D. *J. Pharm. Pharmacol.* **2004**, *56*, 691−702.

(2) (a) Granger, D. N.; Schmid-Schönbein, G. *Physiology and Pathophysiology of Leukocyte Adhesion*; Oxford University Press: New York, 1995; (b) Kansas, G. S. *Blood* **1996**, *88*, 3259−3287.

(3) Gout, S.; Tremblay, P.-L.; Huot, J. *Clin. Exp. Methastasis* **2008**, *25*, 335−344.

(4) Magnani, J. L.; Patton, J. T.; Sarkar, A. K.; Svarovsky, S. A.; Ernst, B. Heterobifunctional Pan-Selectin Inhibitors. Patent WO 2007/028050 A1, priority date: September 2, 2005.

(5) Chang, J.; Patton, J. T.; Sarkar, A.; Ernst, B.; Magnani, J. L.; Frenette, P. S. *Blood* **2010**, *116*, 1779−1786.

(6) *Clinical Trials*; National Institutes of Health: Bethesda, MD; http://clinicaltrials.gov/ct2/results?term=pan-selectin

(7) (a) Phillips, M. L.; Nudelman, E.; Gaeta, F. C. A.; Perez, M.; Singhal, A. K.; Hakomori, S. I.; Paulson, J. C. *Science* **1990**, *250*, 1130−1132. (b) Walz, G.; Aruffo, A.; Kolanus, W.; Bevilacqua, , M.; Seed, B. *Science* **1990**, *250*, 1132−1135.

(8) (a) Binder, F. P. C.; Lemme, K.; Preston, R. C.; Ernst, B. *Angew. Chem., Int. Ed.* **2012**, *51*, 7327−7331. (b) Cooke, R. M.; Hale, R. S.; Lister, S. G.; Shah, G.; Weir, M. P. *Biochemistry* **1994**, *33*, 10591−10596. (c) Poppe, L.; Brown, G. S.; Philo, J. S.; Nikrad, P. V.; Shah, B. H. *J. Am. Chem. Soc.* **1997**, *119*, 1727−1736.

(9) (a) Baumann, K.; Kowalczyk, D.; Gutjahr, T.; Pieczyk, M.; Jones, C.; Wild, M. K.; Vestweber, D.; Kunz, H. *Angew. Chem., Int. Ed.* **2009**, *48*, 3174−3178. (b) Wild, M. K.; Huang, M. C.; Schulze-Horsel, U.; van der Merwe, P. A.; Vestweber, D. *J. Biol. Chem.* **2001**, *276*, 31602−31612.

(10) (a) Sears, P.; Wong, C.-H. *Angew. Chem., Int. Ed.* **1999**, *38*, 2300−2324. (b) Ernst, B.; Kolb, H. C.; Schwardt, O. In *Carbohydrate Mimetics in Drug Discovery*; Levy, D. E., Fügedi, P., Eds.; CRC Press/Taylor & Francis: Boca Raton, 2006, pp 803−845; (c) Kaila, N.; Thomas, B. E. *Med. Res. Rev.* **2002**, *22*, 566−601. (d) Simanek, E. E.; McGarvey, G. J.; Jablonowski, J. A.; Wong, C. H. *Chem. Rev.* **1998**, *98*, 833−862. (e) Kolb, H. C.; Ernst, B. *Chem.—Eur. J.* **1997**, *3*, 1571−1578. (f) Schwizer, D.; Patton, J. T.; Cutting, B.; Smieško, M.; Wagner, B.; Kato, A.; Weckerle, C.; Binder, F. P. C.; Rabbani, S.; Schwardt, O.; Magnani, J. L.; Ernst, B. *Chem.—Eur. J.* **2012**, *18*, 1342−1351.

(11) Copeland, R. A.; Pompliano, D. L.; Meek, T. D. *Nat. Rev. Drug Discovery* **2006**, *5*, 730−739.

(12) (a) Scott, D. E.; Coyne, A. G.; Hudson, S. A.; Abell, C. *Biochemistry* **2012**, *51*, 4990−5003. (b) Coyne, A. G.; Scott, D. E.; Abell, C. *Curr. Opin. Chem. Biol.* **2010**, *14*, 299−307. (c) Chessari, G.; Woodhead, A. J. *Drug Discovery Today* **2009**, *14*, 668−675. (d) Congreve, M.; Chessari, G.; Tisi, D.; Woodhead, A. J. *J. Med. Chem.* **2008**, *51*, 3661−3680. (e) Hajduk, P. J.; Greer, J. *Nat. Rev. Drug Discovery* **2007**, *6*, 211−219. (f) Dalvit, C. *Drug Discovery Today* **2009**, *14*, 1051−1057. (g) Balogh, E.; Wu, D.; Zhou, G.; Gochin, M. *J. Am. Chem. Soc.* **2009**, *131*, 2821−2823. (h) Jhoti, H.; Cleasby, A.; Verdonk, M.; Williams, G. *Curr. Opin. Chem. Biol.* **2007**, *11*, 485−493. (i) Shuker, S. B.; Hajduk, P. J.; Meadows, R. P.; Fesik, S. W. *Science* **1996**, *274*, 1531−1534. (j) Hartshorn, M. J.; Murray, C. W.; Cleasby, A.; Frederickson, M.; Tickle, I. J.; Jhoti, H. *J. Med. Chem.* **2005**, *48*, 403−413. (k) Neumann, T.; Junker, H.-D.; Schmidt, K.; Sekul, R. *Curr. Top. Med. Chem.* **2007**, *7*, 1630−1642.

(13) Jencks, W. *Proc. Nat. Acad. Sci. U.S.A.* **1981**, *78*, 4046−4050.

(14) (a) Finkelstein, A. V.; Janin, J. *Protein Eng.* **1989**, *3*, 1−3. (b) Murray, C. W.; Verdonk, M. L. *J. Comput.-Aided Mol. Des.* **2002**, *16*, 741−753.

(15) (a) Whiting, M.; Muldoon, J.; Lin, Y. C.; Silverman, S. M.; Lindstrom, W.; Olson, A. J.; Kolb, H. C.; Finn, M. G.; Sharpless, K. B.; Elder, J. H.; Fokin, V. V. *Angew. Chem., Int. Ed.* **2006**, *45*, 1435−1439. (b) Krasiński, A.; Radić, Z.; Manetsch, R.; Raushel, J.; Taylor, P.; Sharpless, K. B.; Kolb, H. C. *J. Am. Chem. Soc.* **2005**, *127*, 6686−6692. (c) Mocharla, V. P.; Colasson, B.; Lee, L. V.; Roper, S.; Sharpless, K. B.; Wong, C.-H.; Kolb, H. C. *Angew. Chem., Int. Ed.* **2005**, *44*, 116−120. (d) Lewis, W. G.; Green, L. G.; Grynszpan, F.; Radic, Z.; Carlier, P. R.; Taylor, P.; Finn, M. G.; Sharpless, K. B. *Angew. Chem., Int. Ed.* **2002**, *41*, 1053−1057.

(16) Shelke, S.; Cutting, B.; Jiang, X.; Koliwer-Brandl, H.; Strasser, D.; Schwardt, O.; Kelm, S.; Ernst, B. *Angew. Chem., Int. Ed.* **2010**, *49*, 5721−5725.

(17) Somers, W. S.; Tang, J.; Shaw, G. D.; Camphausen, R. T. *Cell* **2000**, *103*, 467−479.

(18) Otting, G. *Curr. Opin. Struct. Biol.* **1993**, *3*, 760−768.

(19) Jahnke, W.; Perez, L. B.; Paris, C. G.; Strauss, A.; Fendrich, G.; Nalin, C. M. *J. Am. Chem. Soc.* **2000**, *122*, 7394−7395.

(20) Bertini, I.; Fragai, M.; Lee, Y.-M.; Luchinat, C.; Terni, B. *Angew. Chem., Int. Ed.* **2004**, *43*, 2254−2256.

(21) (a) Huisgen, R.; Szeimies, G.; Moebius, L. *Chem. Ber* **1967**, *100*, 2494−2507. (b) Huisgen, R. In *1,3-Dipolar Cycloaddition Chemistry*; Padwa, A., Ed.; Wiley: New York, 1984; Vol.*1*, p 1−176.

(22) Congreve, M.; Carr, R.; Murray, C.; Jhoti, H. *Drug Discovery Today* **2003**, *8*, 876−877.

(23) Hajduk, P. J.; Olejniczak, E. T.; Fesik, S. W. *J. Am. Chem. Soc.* **1997**, *119*, 12257−12261.

(24) (a) Cerichelli, G.; Grande, C.; Luchetti, L.; Mancini, G. *J. Org. Chem.* **1991**, *56*, 3025−3030. (b) Gais, H. J.; Lukas, K. L. *Angew. Chem., Int. Ed. Engl.* **1984**, *23*, 142−143. (c) Roberts, S. M. *Biocatalysts or Fine Chemicals Synthesis*, John Wiley & Sons: Chichester, 1999; (d) Barton, D. H. R.; Crich, D.; Motherwell, W. B. *J. Chem. Soc., Chem. Commun.* **1983**, 939−941. (e) Barton, D. H. R.; Crich, D.; Motherwell, W. B. *Tetrahedron Lett.* **1983**, *24*, 4979−4982.

(25) Sato, S.; Mori, M.; Ito, Y.; Ogawa, T. *Carbohydr. Res.* **1986**, *155*, C6−C10.

(26) Ernst, B.; Wagner, B.; Baisch, G.; Katopodis, A.; Winkler, T.; Öhrlein, R. *Can. J. Chem.* **2000**, *78*, 892−904.
(27) (a) Rich, R. L.; Myszka, D. G. *Curr. Opin. Biotech* **2000**, *11*, 54−61. (b) Morton, T. A.; Myszka, D. G. *Methods Enzymol.* **1998**, *295*, 268−294. (c) Nagata, K.; Handa, H. *Real-Time Analysis of Biomolecular Interactions: Applications of Biacore*; Springer-Verlag: Berlin, 2000.
(28) Bertini, I.; Luchinat, C.; Parigi, G.; Pierattelli, R. *ChemBioChem* **2005**, *6*, 1536−1549.
(29) Safe, S. F. Substituted analogs of indole-3-carbinol and of diindolymethane as antiestrogens. Patent WO9850357 A2; priority date: March 7, 1997; pp 14−15.
(30) Cremlyn, R. J. W. *Aust. J. Chem.* **1973**, *26*, 1591−1593.
(31) Larock, R. C.; Yum, E. K.; Refvik, M. D. *J. Org. Chem.* **1998**, *63*, 7652−7662.
(32) (a) Mamidyala, S. K.; Dutta, S.; Chrunyk, B. A.; Préville, C.; Wang, H.; Withka, J. M.; McColl, A.; Subashi, T. A.; Hawrylik, S. J.; Griffor, M. C.; Kim, S.; Pfefferkorn, J. A.; Price, D. A.; Menhaji-Klotz, E.; Mascitti, V.; Finn, M. G. *J. Am. Chem. Soc.* **2012**, *134*, 1978−1981. (b) Rillahan, C. D.; Schwartz, E.; McBride, R.; Fokin, V. V.; Paulson, J. C. *Angew. Chem., Int. Ed.* **2012**, *51*, 11014−11018.
(33) (a) Rostovtsev, V. V.; Green, L. G.; Fokin, V. V.; Sharpless, K. B. *Angew. Chem., Int. Ed.* **2002**, *41*, 2596−2599. (b) Tornoe, C. W.; Christensen, C.; Meldal, M. *J. Org. Chem.* **2002**, *67*, 3057−3064.
(34) Lu, H.; Tonge, P. J. *Curr. Opin. Chem. Biol.* **2010**, *14*, 467−474.
(35) Vedani, A.; Dobler, M.; Smiesko, M. *Toxicol. Appl. Pharmacol.* **2012**, *261*, 142−153.
(36) Macherey, A.-C.; Dansette, P. M. In *Chemical mechanisms of toxicity: Basic knowledge for designing safer drugs*; Wermuth, C. G., Ed.; Elsevier Academic Press: Amsterdam, 2003, pp 545−560.
(37) (a) Paulini, R.; Müller, K.; Diederich, F. *Angew. Chem., Int. Ed.* **2005**, *44*, 1788−1805. (b) Robinson, J. M. A.; Philp, D.; Harris, K. D. M.; Kariuki, B. M. *New J. Chem.* **2000**, *24*, 799−806. (c) Abraham, M. H.; Duce, P. P.; Prior, D. V.; Barratt, D. G.; Morris, J. J.; Taylor, P. J. *J. Chem. Soc., Perkin Trans. 2* **1989**, 1355−1375. (d) Panunto, T. W.; Urbanczyk-Lipkowska, Z.; Johnson, R.; Etter, M. C. *J. Am. Chem. Soc.* **1987**, *109*, 7786−7797.
(38) Cabani, S.; Gianni, P.; Mollica, V.; Lepori, L. *J. Solution Chem.* **1981**, *10*, 563−595.
(39) Hwang, T.-L.; Shaka, A. J. *J. Magn. Reson. A* **1995**, *112*, 275−279.
(40) Cutting, B.; Shelke, S. V.; Dragic, Z.; Wagner, B.; Gathje, H.; Kelm, S.; Ernst, B. *Magn. Reson. Chem.* **2007**, *45*, 720−724.
(41) Mesch, S.; Lemme, K.; Koliwer-Brandl, H.; Strasser, D. S.; Schwardt, O.; Kelm, S.; Ernst, B. *Carbohydr. Res.* **2010**, *345*, 1348−1359.
(42) Frostell-Karlsson, A.; Remaeus, A.; Roos, H.; Andersson, K.; Borg, P.; Hamalainen, M.; Karlsson, R. *J. Med. Chem.* **2000**, *43*, 1986−1992.
(43) Jahnke, W.; Kolb, H. C.; Blommers, M. J. J.; Magnani, J. L.; Ernst, B. *Angew. Chem., Int. Ed. Engl.* **1997**, *36*, 2603−2607.